Anions coordinating anions: Analysis of the interaction between anionic Keplerate nanocapsules and their anionic ligands

Dolores Melgar,[a,b] Nuno A. G. Bandeira,[a,c,d] Josep Bonet Avalos,[b] Carles Bo*[a,e]

Keplerates are a family of anionic metal oxide spherical capsules containing up to 132 metal atoms and some hundreds of oxygens. These capsules holding a high negative charge of -12 coordinate both mono-anionic and di-anionic ligands thus raising its charge till -42 even till -72, which is compensated by the corresponding counter-cations in X-Ray structures. We present an analysis of the relative importance of several energy terms of the coordinate bond between the capsule and ligands like carbonate, sulphate, sulphite, phosphinate, selenate, and a variety of carboxylates, of which the overriding component is the contribution due to solvation/de-solvation effects.

Introduction

During the last decade, polyoxometalate (POM) chemistry enabled growing impressive new giant molecular metal oxide nanostructures.[1, 2] In some cases, the shape of the POM framework is such that it forms inner cavities, which are usually filled with other molecular species. These two characteristics are found in the unique family of compounds known as Keplerates, which are uniquely symmetric spherical capsules containing either 102 or 132 metal atoms (Fig. 1).[3, 4] The first discovered and most relevant member of this family is known as Mo_{132} and it was reported by Müller and co-workers in 1998.[5] With general formula $[(Mo^{VI}(Mo^{VI})_5O_{21}(H_2O)_6)_{12}(Mo^{V}_2(\mu\text{-}O)_2O_2(L^{n-}))_{30}]^{(12+n)-}$, where L^{n-} is a bridging anionic ligand, the sphere is highly negatively charged, holding a charge of -42 for monovalent anions (L^-) and -72 for divalent anionic ligands (L^{2-}). This sort of capsule is built from twelve pentagonal $Mo^{VI}(Mo^{VI})_5O_{21}$ units, which are placed at the vertices of an icosahedron and contain six Mo^{VI} atoms. These units are connected by $(Mo_2(\mu\text{-}O)_2O_2(L^{n-})$ dimers or linkers, holding Mo^{V} atoms thus thirty of them are needed to complete the spherical capsule. This building-block combination is highlighted in Fig. 1. In a simplified notation, we will refer to this species as Mo_{132} for short.

Since the initial synthesis of Mo_{132}, Müller and co-workers noticed that other combinations of pentagons and linkers could be possible, and readily discovered $Mo_{72}Fe_{30}$,[6] a Keplerate with $Mo(Mo)_5$ pentagonal units and magnetic Fe^{III} ions as linkers, and a related $Mo_{75}V_{20}$ capsule.[7] The Mo_{102} Keplerate was synthesised next,[8] which is formally a $Mo_{72}Mo_{30}$ Keplerate, incorporating MoO^{3-} groups as linkers. Using the same strategy, the $Mo_{72}V_{30}$ containing $V^{IV}O$ units as linkers[9] and the $Mo_{72}Cr_{30}$ with Cr^{III} linkers[10] were discovered. The next advance was the ability to generate pentagonal units with tungsten centres, i.e., $W(W)_5$ building blocks, that were assembled using both dimeric and monoatomic linkers. Thus, the $W_{72}Mo_{60}$[11] and $W_{72}Fe_{30}$[12] clusters were discovered. Further chemical synthesis enabled replacing μ-oxo with μ-thio bridging ligands in the $Mo^{V}_2(\mu\text{-}S)_2O_2$ linker moiety within the frameworks of $W_{72}Mo_{60}(\mu\text{-}S)_2$[13] and $Mo_{132}(\mu\text{-}S)_2$,[14] and the mixed μ-oxo/thio bridges, such as $Mo^{V}_2(\mu\text{-}O)(\mu\text{-}S)O_2$ introduced in the $W_{72}Mo_{60}$ cluster.[15]

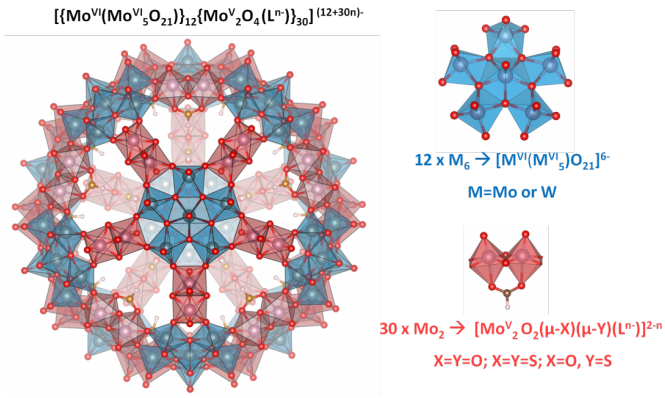

Fig. 1 Polyhedral representation of Mo_{132} (left) with formate groups acting as the ligands bound to the interior wall of the linkers. The two types of building blocks have been highlighted (right): blue for the pentagonal (Mo^{VI}) units and red for the dimeric (Mo^{V}) linkers.

In Keplerates, the ligands L in the linker units [$Mo^{V}_2(\mu\text{-}X)_2O_2(L^{n-})$, X=O, S] are bidentate oxygen donor anions such as formate,[16-18] acetate,[4, 5] monochloroacetate,[18] sulphate,[4, 19, 20] sulphite,[21] hipophosphite,[6, 22] hydrogen phosphate,[19] selenate,[23] valerate,[24] carbonate,[25] carboxylates in general,[26-29] and even dicarboxylates.[30] Some of these can undergo rapid exchange with others either internally or by transiting through the pores of the Keplerate.[31] From a pure electrostatic point of view, it seems non rational that a large number (30 units) of anionic ligands (charge –1, –2) coordinate to an anionic capsule $[(Mo^{VI}(Mo^{VI})_5O_{21}(H_2O)_6)_{12}(Mo^{V}_2(\mu\text{-}O)_2O_2)_{30}]^{12-}$, which formally holds a high negative charge. The whole system raises then its charge from –12 to –42, or even to –72 upon ligand coordination, which is compensated by the corresponding counter-cations (either inside or outside the capsule).

For a series of similar carboxylates, it has been demonstrated that the exchange rate through the pores depends on the size of the carboxylate substituent.[26] The hydrophobic environment generated by propionate ligands allowed the encapsulation of 1-hexanol,[27] and when longer carbon chains were introduced, as in n-Pr-CO_2^- carboxylates, they self-assemble step-wise inside the capsule.[28] Capsules internally decorated with propionate ligands can selectively distinguish hydrophobic domains by sequestering differently sized alkanes (from n-heptane to methane).[32]

The dynamic nature of Keplerate-ligand interactions from this inside/outside exchange of molecular species suggested the possibility that these nanoclusters could purposefully also be used as nanoreactors. The first properly identified application of Mo_{132} as a nanoreactor was found in the hydrolysis of methyl tert-butyl ether, a reaction that takes place inside the capsule and it is mediated by the $Mo^{V}_2(\mu\text{-}O)_2O_2$ linkers as DFT based studies by some of us and detailed NMR experiments demonstrated.[33] Mo_{132} has shown to be also capable of modifying the regioselectivity of the Huisgen reaction,[34] and very remarkably, to uptake CO_2 and transform it to carbonate.[25] The mechanism of this CO_2 hydration reaction is now well understood and is mediated by the linkers too.[35] Related to CO_2 uptake, Garai *et al.* recently reported the transformation of SO_2 gas into SO_3^{2-} ligands.[21] Other examples of the catalytic activity of Keplerates all fall in the category of oxidation reactions, which in our opinion probably occur outside the capsule. [36-45]

Some issues regarding Keplerate chemistry were addressed computationally using both classical and quantum methods. Our group demonstrated[46] that the layered structure of encapsulated water could be reproduced using molecular dynamics simulations, and studied its dynamic behaviour.[47, 48] Other authors studied the assembly of Keplerates in sheet-like structures using Monte Carlo methods.[49, 50] Our group used DFT methods to study catalytic reaction mechanisms by considering models of the capsules,[33, 35] and described for the first time the electronic structure of Mo_{132} and $W_{72}Mo_{60}$.[25] Kuepper *et al.* discussed the electronic structure of $Mo_{72}Fe_{30}$ and $W_{72}Fe_{30}$.[51]

Since anionic ligands coordinating to an already anionic Keplerate appears paradoxical, and given the key role that Keplerate-ligand interactions play in tuning the chemical properties of the inner surface of these capsules, in this manuscript we are reporting a detailed study of the interaction between the Mo_{132} capsule and different types of ligands. The analysis relies on the bonding energy decomposition analysis (EDA).[52-58] The procedure we used enables decomposing the energy changes upon bonding of two molecular fragments in several energy terms, namely Pauli, electrostatic, orbital interactions, and solvation energy balance.

The EDA procedure has been widely employed to analyse the nature of the bonding between molecular fragments in a variety of cases,[59, 60] including interactions between transition metal atoms and ligands of a varied nature.[61] In most of these examples, a non-charged system was divided into neutral fragments, and the analysis did not take into consideration any sort of solvent effects.[60] Other examples can be found in which charged fragments interact to form either a neutral[62, 63] or a charged system,[64, 65] but in these cases solvent effects were

not included in the analysis either. De Jong and Bickelhaupt[66] introduced for the first time the EDA analysis in solvent, thus we followed an equivalent protocol. In a very recent example that dealt with a host-guest charged system, supramolecular interactions including solvent effects were analysed in terms of EDA.[67] Since including solvent effects within the EDA framework is not a straightforward protocol, we describe herein a general procedure for extracting the relevant data.

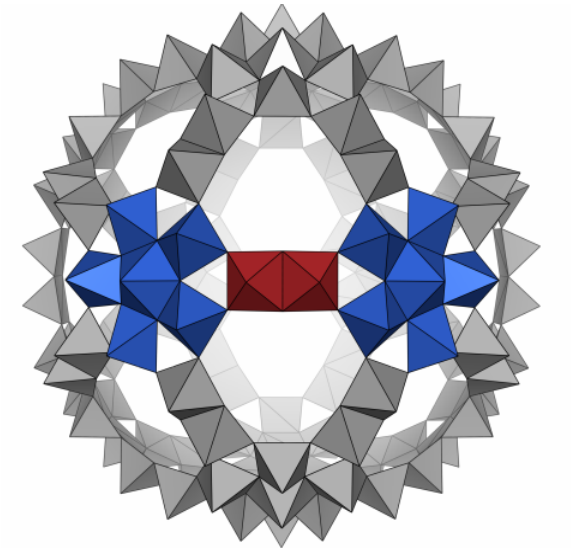

Fig. 2 A fragment cut-out of the $[(Mo^{VI}_{6}O_{21})_2(Mo^{V}_{2}O_4)]^{10-}$ simplified model ion used in the calculations (blue for pentagons and red for the linker).

In this paper, we consider various charged fragments that form a charged system, taking into account the role of the solvent by means of a continuum model. The relationship between the computed bonding energies and the pK_b of anionic ligands sets up the basis to understanding Keplerate-ligand interactions.

Computational Details and Models

All the results presented herein were obtained using the ADF2012 program system.[52, 68] The BP86[69-71] DFT GGA functional including scalar relativistic ZORA[72, 73] approach was used together with the Slater triple-ζ plus polarization basis sets (TZP) in all atoms, which included frozen cores up to 4p for Mo and 1s for O and C atoms. Solvent effects were introduced non-explicitly by means of the COSMO model.[74, 75] The values of the atomic radii correspond to the Van der Waals radii from the MM3 method developed by Allinger.[76] A data set collection of input and output files is available online[77] in the ioChem-BD repository. [78]
The energy decomposition analysis (EDA) as implemented in ADF was applied to divide the bonding energy between the capsule and its ligands into four parts: the Pauli repulsion, the electrostatic energy, the orbital interaction energy and finally the solvation energy contribution. Given the anionic nature of both the capsule and the ligands, the latter plays a key factor in balancing out excessive electrostatic and bonding repulsions. The electrostatic interaction component yields the classical electrostatic contribution between the unperturbed fragments and the Pauli repulsion term is the anti-symmetrisation energy penalty (always positive) between electrons of like spin upon assembling the two fragments. Neither of these components changes upon inclusion of implicit solvation models. Only the orbital interaction term, which is a consequence of the relaxation due to overlapping the two fragment densities, is different with the use of COSMO with respect to the *in vacuo* orbital interaction term, since there is an intrinsic change in electronic density due to the solvation potential. The deformation energies of the ligands were computed in the case of the full capsule model, and taken into account in the final total bonding energy value.

The outcome of EDA is largely dependent on how fragments are defined. In the present case, and following our successful previous experience in studying chemical reactions catalysed by Mo_{132},[33, 35] a first choice would be one linker unit and two capping pentagon moieties, highlighted in Fig. 2, as a model of the whole capsule. This would be justified as a compromise between accurate chemical description and computational cost. But doing that, the degree of protonation to saturate the dangling bonds introduces additional uncertainties, since this model system might be fully protonated as in $[(H_8Mo^{VI}_{6}O_{21})_2(Mo^{V}_{2}O_4)]^{6+}$, or fully deprotonated as in the $[(Mo^{VI}_{6}O_{21})_2(Mo^{V}_{2}O_4)]^{10-}$ anionic fragment. Although both models retain the main characteristics of the linker's chemical environment, the presence or lack of protons in the pentagon motifs make the whole model either highly positively or highly negatively charged. Actually, the anionic model is closer to the actual charge if we consider the whole capsule $[(Mo^{VI}_{6}O_{21})_{12}(Mo^{V}_{2}O_4)_{30}]^{12-}$. We considered notwithstanding these three models: the two models of the linker unit interacting with one ligand, and the entire thirty ligands being bound onto the capsule walls. We are

presenting herein the results for the anionic model and the whole capsules, whereas the results for the cationic model are included in the Supporting Information.

Since the EDA implementation requires the fragments to be in the gas-phase, the energy that ADF provides in such kind of analysis is ΔE_{sol}^{frag}, as indicated in the thermodynamic cycle in Scheme 1.

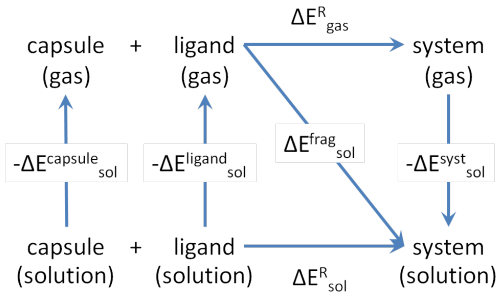

Scheme 1 Definition and notation of the different energies terms in the thermodynamic cycle.

To compute the Bonding Energy, which we label as ΔE_{sol}^{R} in Scheme 1, we could use Equation 1.

$$\Delta E_{sol}^{R} = E_{sol}^{syst} - E_{sol}^{capsule} - E_{sol}^{lig} \qquad (1)$$

When the EDA is carried out using ADF, the magnitude ΔE_{sol}^{frag} is obtained (Equation 2).

$$\begin{aligned} \Delta E_{sol}^{frag} &= E_{sol}^{syst} - E_{gas}^{capsule} - E_{gas}^{lig} = \\ &= \left(E_{sol}^{syst} - E_{gas}^{syst}\right) + \left(E_{gas}^{syst} - E_{gas}^{capsule} - E_{gas}^{lig}\right) = \\ &= \Delta E_{sol}^{syst} + \Delta E_{gas}^{R} \end{aligned} \qquad (2)$$

The combination of (1) and (2) give Equation 3. Note that $E_{sol}^{i} - E_{gas}^{i}$ is the solvation energy of species i.

$$\Delta E_{sol}^{R} = \Delta E_{sol}^{frag} + \left(E_{gas}^{capsule} - E_{sol}^{capsule}\right) + \left(E_{gas}^{lig} - E_{sol}^{lig}\right) \qquad (3)$$

Of course, we can also compute ΔE_{sol}^{R} directly, just evaluating the energy in solution of the whole system and of the fragments to know E_{sol}^{sys}, $E_{gas}^{capsule}$ and E_{gas}^{lig} as in Equation 1. But since we aim at decomposing the interaction energy between the two fragments under the EDA framework, we used the fragment based approach leading thus to Equation 4.

$$\Delta E_{sol}^{R} = \Delta E_{gas}^{R} + \Delta E_{sol}^{syst} - \Delta E_{sol}^{capsule} - \Delta E_{sol}^{lig} \qquad (4)$$

The two approaches give fully equivalent results. The reader can find a detailed numerical example in the Supporting Information.

Results and discussion

$[(Mo^{VI}_6O_{21})_2(Mo^{V}_2O_4)]^{10-}$ Model. By following the procedure described above, we considered a model of the capsule, i.e. the negatively charged fragment $[(Mo^{VI}_6O_{21})_2(Mo^{V}_2O_4)]^{10-}$. The two pentagonal moieties are joined together with a linker unit, without any additional protons, exactly as highlighted in Fig. 2. Note that the model holds a high negative charge, which is much larger than in the real system. Table 1 collects the decomposition of the energy bonding terms obtained from the EDA analysis and the differences in solvation energy.

Table 1 Bonding energy decomposition in eV of the interaction between the $[(Mo^{VI}_6O_{21})_2(Mo^{V}_2O_4)]^{10-}$ model and various ligands.

	SeO_4^{2-}	SO_4^{2-}	SO_3^{2-}	HSO_4^{-}	CO_3^{2-}
Pauli Repulsion	8.04	7.49	9.47	4.43	11.96
Electrost. Int.	24.95	25.63	24.29	12.73	21.97
Orbital Int.	-5.65	-5.59	-7.18	-2.33	-9.52

Diff. Solvation Energy	-28.25	-28.33	-28.29	-15.00	-26.88
Bonding Energy	**-0.91**	**-0.79**	**-1.71**	**-0.18**	**-2.47**

	HCO_3^-	$HCOO^-$	CH_3COO^-	$H_2PO_2^-$
Pauli Repulsion	5.79	5.96	6.36	6.99
Electrost. Int.	11.91	11.74	11.33	11.19
Orbital Int.	-3.15	-3.22	-3.30	-3.55
Diff. Solvation Energy	-15.40	-15.47	-15.53	-15.66
Bonding Energy	**-0.85**	**-0.99**	**-1.16**	**-1.03**

As expected, the electrostatic energy between the unperturbed charge densities of the two anions (model and ligand) shows positive values in all the cases. The magnitude of the electrostatic term follows a clear trend dictated by the charge of the ligand, di-anionic ligands roughly doubling the repulsion computed for mono-anionic ligands. The difference in solvation energy follows a very similar trend dictated by the ligand charge, although this term is clearly stabilizing. This is because the total charge of the system increases upon bonding. Actually, the whole system is more charged (-11 or -12) than its fragments (-1 or -2, and -10), so solvation energy differences contribute to bonding. Since the Pauli repulsion term is positive in all cases, it is the balance between the orbital interactions and the solvation energy, compared to the repulsive terms, which makes the total bonding energies negative. It is worth noting that although individual terms afford high numbers in absolute value, the total bonding energies are negative in all the cases and relatively small. Again, mono-anionic ligands are less strongly bound to the linker unit than di-anionic ligands, apart from SO_4^{2-} and SeO_4^{2-}. We will discuss this apparently wrong trend below. A close look at the values in Table 1 reveals that it is not only the charge of the ligand what determines the bonding strength, but the chemical nature of the different ligands. At this point, it is worth noting that the most strongly bound ligand, carbonate CO_3^{2-} and sulphite SO_3^{2-}, are precisely the products obtained in the related catalytic transformations reported recently.[21, 25, 35]

We carried out the same analysis for a series of carboxylate ligands as shown in Fig. 3. The results we obtained are collected in Table 2. As expected, no surprises arise from these results, just confirming the similarity between the bonding properties of these ligands. Differences are really small in all cases, so in line with ligand exchange experiments. Note that despite the high negative charge of the model we chose for the cluster, bonding energies of anionic ligands are negative in all the cases resulting in favourable bonding.

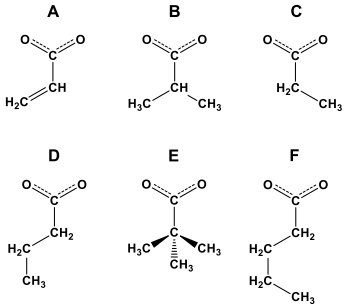

Fig. 3 A series of carboxylate ligands: acrylate, isobutyrate, propionate, butyrate, pivalate, and pentanoeate. We will refer to these species as A, B, C, D, E, and F for short.

Table 2 Bonding energy decomposition in eV of the interaction between the $[(Mo^{VI}_6O_{21})_2(Mo^{V}_2O_4)]^{10-}$ model and various ligands with different carbon chains. Labels meanings are indicated on Fig. 3.

	A	**B**	**C**	**D**	**E**	**F**
Pauli Repulsion	6.43	6.69	6.36	6.53	6.73	6.50
Electrost. Int.	11.27	10.92	11.24	11.03	10.84	10.97
Orbital Int.	-3.16	-3.28	-3.24	-3.23	-3.26	-3.14
Diff. Solv. Energy	-15.64	-15.43	-15.52	-15.49	-15.36	-15.50
Bonding Energy	**-1.11**	**-1.10**	**-1.17**	**-1.16**	**-1.04**	**-1.17**

We refer the reader to the Supporting Information section where we included the results of a similar analysis on a model of the capsule which is a fully protonated and positively charged fragment $[(H_8Mo^{VI}_6O_{21})_2(Mo^{V}_2O_4)]^{6+}$. As expected, for such a model, the total bonding

energies values are much more negative than for the $[(Mo^{VI}_6O_{21})_2(Mo^{V}_2O_4)]^{10-}$ model since the electrostatic term predominates. Solvation energy differences, however, play an opposite role. From the results here gathered it is clearly revealed that the EDA is strongly dependent on the model, the sign of electrostatic and the solvation energy terms being highly dependent on the charge of the fragment chosen. However, it is worth mentioning that the same trends amongst the ligands are obtained, independently of the model.

$[(Mo^{VI}_6O_{21})_{12}(Mo^{V}_2O_4)_{30}]^{12-}$ Capsule. To eliminate ambiguities, we applied the same procedure as described above and considered the full capsule coordinating 30 ligands, in order to compare with the results provided by the two aforementioned smaller models. Instead of taking into account just a Mo_{132} fragment, we dealt with the whole Mo_{132} capsule and computed and decomposed the total bonding energy between the Keplerate and its 30 ligands decorating the inner surface of the capsule. Results are collected in Table 3 and Fig. 4. In this case we have also accounted for the ligands deformation energy, which is the energy needed to bring a ligand from solution to coordinating to the linkers within the capsule.

Table 3 Bonding energy decomposition in eV of the interaction between the Mo_{132} capsule and the 30 inner ligands. Values for the whole system and per ligand.

	SeO_4^{2-}	SO_4^{2-}	SO_3^{2-}	HSO_4^-	CO_3^{2-}
Pauli Repulsion	275.84	235.17	289.10	110.10	295.09
Pauli Rep. / ligand	9.19	7.84	9.64	3.67	9.84
Electrost. Interaction	262.16	298.54	239.14	182.34	232.79
Electrost. Int. / ligand	8.74	9.95	7.97	6.08	7.76
Orbital Interaction	-420.87	-379.79	-461.25	-139.92	-442.13
Orbital Int. / ligand	-14.03	-12.66	-15.37	-4.66	-14.74
Diff. Solvation Energy	-129.91	-141.00	-98.71	-145.69	-116.46
Diff. Solv. E / ligand	-4.33	-4.70	-3.29	-4.86	-3.88
Bonding Energy	-12.78	-5.17	-31.72	6.83	-30.71
BE / ligand	**-0.43**	**-0.17**	**-1.06**	**0.23**	**-1.02**
Deform. E / ligand	0.27	0.08	0.09	0.03	0.04
Total BE / ligand	**-0.15**	**-0.09**	**-0.96**	**0.26**	**-0.98**

	HCO_3^-	$HCOO^-$	CH_3COO^-	CH_2CHCOO^-	$H_2PO_2^-$
Pauli Repulsion	148.79	152.05	172.67	186.02	167.25
Pauli Rep. / ligand	4.96	5.07	5.76	6.20	5.58
Electrost. Interaction	136.14	134.62	113.77	102.33	118.50
Electrost. Int. / ligand	4.54	4.49	3.79	3.41	3.95
Orbital Interaction	-65.34	-158.27	-168.89	-172.87	-164.61
Orbital Int. / ligand	-2.18	-5.28	-5.63	-5.76	-5.49
Diff. Solvation Energy	-139.02	-144.52	-136.25	-131.70	-139.05
Diff. Solv. E / ligand	-4.63	-4.82	-4.54	-4.39	-4.64
Bonding Energy	-25.09	-16.12	-18.70	-16.23	-17.91
BE / ligand	**-0.84**	**-0.54**	**-0.62**	**-0.54**	**-0.60**
Deform. E / ligand	0.01	0.00	0.01	0.01	0.01
Total BE / ligand	**-0.82**	**-0.53**	**-0.62**	**-0.53**	**-0.59**

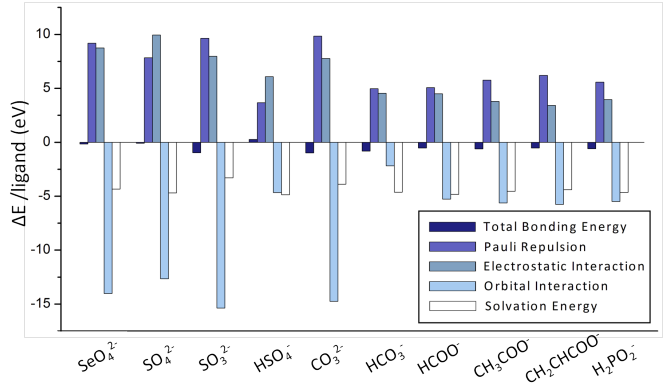

Fig. 4 Bonding energies per ligand in eV with its decomposition into the different energy terms for the interaction of the Mo_{132} capsule with a set of bidentate ligands.

Results in Table 3 and Fig. 4 show that the sign of each individual contribution to the total bonding energy is equivalent to those obtained when we analysed the negatively charged model $[(Mo^{VI}_6O_{21})_2(Mo^{V}_2O_4)]^{10-}$, namely, negative value for the difference in solvation energy and positive value for the electrostatic interaction term. Note that the Pauli repulsion term almost matches the values obtained with the smaller models, being the origin of the differences tiny changes in the geometrical parameters upon bonding. A remarkable result from Table 3 is that the difference in solvation energy depends on the charge of the ligand in a lesser extend than in the smaller models. This is

because of the smaller charge density in the entire capsule compared to smaller model. Although the total charge of the former is -12, the much larger molecular surface of the capsule with respect to the smaller models attenuates the differences per ligand upon bonding, which was responsible for the large solvation effects observed in the models. Being electrostatic interactions much smaller and solvation/de-solvation effects almost constant along the ligand series, the orbital interaction term plays the main role in the bonding.

Regarding the deformation energy of the ligands, in most of the cases this term contributes less than 10% to the bonding energy. Only for selenate and sulphate, the deformation contribution represents a large percentage of the bonding energy, 63% and 47% respectively. The deformation energy can be understood in terms of the geometrical changes of the ligands upon coordination. For instance, the geometry of the free carbonate ligand (which has a deformation energy contribution of only 4%) is almost exactly the same than when it is coordinated within the capsule. The distance between the oxygen atoms of an acetate ligand increases less than 0.01 Å upon coordination. In contrast, the changes upon bonding for sulphate and selenate are much larger. Particularly the O-O distance between the coordinated oxygen atoms in the selenate ligand increases from 2.766 Å (free) to 2.920 Å (coordinated). This change justifies the largest deformation energy of the selenate ligand, and also the multiple bonding modes found in the X-Ray structures.

The total bonding energy values are smaller in absolute value, which is in agreement with experimental evidence. The equilibrium observed between ligands inside/outside must be originated by relatively small bonding energies, so the values in Table 3 are in line with this. Sulphite and carbonate are the most strongly bound ligands, and, according to the results in Table 3, HSO_4^- would not even coordinate to the capsule. All the tested di-anionic ligands but sulphate are definitively more tightly bound to the capsule than mono-ionic ligands. Again, we obtained an apparently wrong behaviour for the sulphate and selenate anion. However, this trend retains the chemical nature of sulphate anion being a weak base or a weak coordinating ligand. Actually if we plot the computed bonding energy per ligand together with the ligands' experimental pK_b values, some degree of correlation emerges (see Fig. 5). Although EDA provides very large values for some individual components (Pauli repulsion, electrostatic energy) and the balance of solvation effects upon bonding are not negligible, the bonding between the Keplerate capsule and its ligands is mainly dominated by the intrinsic nature of the ligands, hence by their acid/base properties.

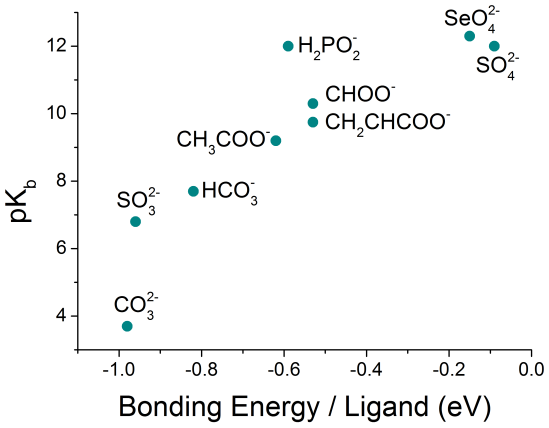

Fig. 5 Correlation between the total bonding energies per ligand and the pK_b values[79, 80] for the set of ligands collected in Table 3.

Conclusions

In summary, we carried out studies on the interaction between the Mo_{132} capsule and its inner ligands by considering two models of the linker with different protonation states, and also the whole capsule as it is. The three models provide similar trends regarding the bonding energy of the ligands, although the results obtained with a negatively charged model are more consistent with the results for the full system. The trends in Keplerate-ligands bond strength are the same for both cases, being carbonate and sulphite the most strongly bound ligands, followed by CH_3COO^-, $H_2PO_2^-$, CH_2CHCOO^-, $HCOO^-$, HCO_3^-, SeO_4^{2-} and finally SO_4^{2-}. This order is in good agreement with experimental observations, and it shows some correlation with the pK_b values of the ligands.

The bonding energy including solvent effects was decomposed by means of EDA method and has been analysed for the three models proposed ($[(H_8Mo^{VI}_6O_{21})_2(Mo^V_2O_4)]^{6+}$, $[(Mo^{VI}_6O_{21})_2(Mo^V_2O_4)]^{10-}$ and the complete Mo_{132} capsule). The decomposition energy analysis is strongly dependent on the model used. In the case of the $[(H_8Mo^{VI}_6O_{21})_2(Mo^V_2O_4)]^{6+}$ model, the bonding energy trends observed were dominated by the electrostatic interaction and the favourable orbital interaction term, because the whole system (model + ligand) is less charged that its fragments. For the $[(Mo^{VI}_6O_{21})_2(Mo^V_2O_4)]^{10-}$ model, the electrostatic interaction and the difference on solvation energies

has an opposing sign compared with the positively charged model, because in this case, the whole system (model + ligand) is more charged than its fragments. In the case of the negatively charged model, it has been shown that even for such a high negative charge cluster, the bonding energies for the set of ligands studied are negative as well.

Finally, we have shown that even the capsule being a large macro-anion, it interacts favourably with negatively charged ligands, and forms not very strong bonds, which are labile in all cases. The interaction of the ligands and the Mo(V) centers in the linker units is dominated by orbital interactions that reflect the chemical nature of the ligands. The pK_b of the ligands correlates almost linearly with the bonding energy.

Acknowledgements

The authors acknowledge the ICIQ Foundation, the Spanish Ministerio de Economía y Competitividad (MINECO) through project CTQ2014-52824-R and the Severo Ochoa Excellence Accreditation 2014-2018 (SEV-2013-0319), and the AGAUR of Generalitat de Catalunya through project 2014-SGR-409 for financial support, and through the CERCA Programme. DM gratefully acknowledges URV-ICIQ fellowship. NAGB gratefully a Fundação para a Ciência e Tecnologia (grant SFRH/BPD/110419/2015) for funding.

Notes and references

1. A. Muller and P. Gouzerh, *Chem. Soc. Rev.*, 2012, **41**, 7431-7463.
2. H. N. Miras, J. Yan, D.-L. Long and L. Cronin, *Chem. Soc. Rev.*, 2012, **41**, 7403-7430.
3. A. Müller, P. Kögerler and A. W. M. Dress, *Coord. Chem. Rev.*, 2001, **222**, 193-218.
4. A. Müller, E. Krickemeyer, H. Bögge, M. Schmidtmann, B. Botar and M. O. Talismanova, *Angew. Chem. Int. Ed.*, 2003, **42**, 2085-2090.
5. A. Müller, E. Krickemeyer, H. Bögge, M. Schmidtmann and F. Peters, *Angew. Chem. Int. Ed.*, 1998, **37**, 3360-3363.
6. A. Müller, S. Sarkar, S. Shah, H. Bögge, M. Schmidtmann, P. Kögerler, B. Hauptfleisch, A. Trautwein and V. Schünemann, *Angew. Chem. Int. Ed. Engl.*, 1999, **38**, 3238-3241.
7. A. Müller, M. Koop, H. Bögge, M. Schmidtmann, F. Peters and P. Kögerler, *Chem. Commun.*, 1999, 1885-1886.
8. A. Müller, S. Shah, H. Bögge, M. Schmidtmann, P. Kögerler, B. Hauptfleisch, S. Leiding and K. Wittler, *Angew. Chem. Int. Ed. Engl.*, 2000, **39**, 1614-1616.
9. A. Müller, A. M. Todea, J. van Slageren, M. Dressel, H. Bögge, M. Schmidtmann, M. Luban, L. Engelhardt and M. Rusu, *Angew. Chem. Int. Ed.*, 2005, **44**, 3857-3861.
10. A. M. Todea, A. Merca, H. Bögge, J. van Slageren, M. Dressel, L. Engelhardt, M. Luban, T. Glaser, M. Henry and A. Müller, *Angew. Chem. Int. Ed.*, 2007, **46**, 6106-6110.
11. C. Schäffer, A. Merca, H. Bögge, A. M. Todea, M. L. Kistler, T. Liu, R. Thouvenot, P. Gouzerh and A. Müller, *Angew. Chem. Int. Ed.*, 2008, **48**, 149-153.
12. A. M. Todea, A. Merca, H. Bögge, T. Glaser, J. M. Pigga, M. L. K. Langston, T. Liu, R. Prozorov, M. Luban, C. Schröder, W. H. Casey and A. Müller, *Angew. Chem. Int. Ed.*, 2009, **49**, 514-519.
13. C. Schäffer, A. M. Todea, H. Bögge, E. Cadot, P. Gouzerh, S. Kopilevich, I. A. Weinstock and A. Müller, *Angew. Chem. Int. Ed.*, 2011, **50**, 12326-12329.
14. F. Bannani, S. Floquet, N. Leclerc-Laronze, M. Haouas, F. Taulelle, J. Marrot, P. Kögerler and E. Cadot, *J. Am. Chem. Soc.*, 2012, **134**, 19342-19345.
15. C. Schäffer, A. M. Todea, H. Bögge, S. Floquet, E. Cadot, V. S. Korenev, V. P. Fedin, P. Gouzerh and A. Müller, *Dalton Trans.*, 2012, **42**, 330.
16. A. Muller, K. Das, E. Krickemyer and C. Kuhlmann, *Inorganic synthesis*, 2004, **34**, 191-200.
17. A. Proust, R. Thouvenot and P. Gouzerh, *Chem. Commun.*, 2008, 1837-1852.
18. A. Müller, V. P. Fedin, C. Kuhlmann, H. Bögge and M. Schmidtmann, *Chem. Commun.*, 1999, 927-929.
19. A. Müller, S. K. Das, S. Talismanov, S. Roy, E. Beckmann, H. Bögge, M. Schmidtmann, A. Merca, A. Berkle, L. Allouche, Y. Zhou and L. Zhang, *Angew. Chem. Int. Ed.*, 2003, **42**, 5039-5044.
20. A. Müller, E. Krickemeyer, H. Bögge, M. Schmidtmann, S. Roy and A. Berkle, *Angew. Chem. Int. Ed.*, 2002, **41**, 3604-3609.
21. S. Garai, M. Rubčić, H. Bögge, P. Gouzerh and A. Müller, *Chem. Eur. J.*, 2015, **21**, 4321-4325.
22. V. Béreau, E. Cadot, H. Bögge, A. Müller and F. Sécheresse, *Inorg. Chem.*, 1999, **38**, 5803-5808.
23. V. S. Korenev, P. A. Abramov, C. Vicent, A. A. Zhdanov, A. R. Tsygankova, M. N. Sokolov and V. P. Fedin, *Dalton Trans.*, 2015, **44**, 8839-8845.
24. S. Garai, H. Bögge, A. Merca, O. A. Petina, A. Grego, P. Gouzerh, E. T. K. Haupt, I. A. Weinstock and A. Müller, *Angew. Chem. Int. Ed.*, 2016, **55**, 6634-6637.
25. S. Garai, E. T. K. Haupt, H. Bögge, A. Merca and A. Müller, *Angew. Chem. Int. Ed.*, 2012, **51**, 10528-10531.
26. A. Ziv, A. Grego, S. Kopilevich, L. Zeiri, P. Miro, C. Bo, A. Müller and I. A. Weinstock, *J. Am. Chem. Soc.*, 2009, **131**, 6380-6382.
27. C. Schäffer, A. M. Todea, H. Bögge, O. A. Petina, D. Rehder, E. T. K. Haupt and A. Müller, *Chem. Eur. J.*, 2011, **17**, 9634-9639.

28. A. Grego, A. Müller and I. A. Weinstock, *Angew. Chem. Int. Ed.*, 2013, **52**, 8358-8362.
29. A. Muller, L. Toma, H. Bogge, M. Henry, E. T. K. Haupt, A. Mix and F. L. Sousa, *Chem. Commun.*, 2006, 3396-3398.
30. T.-L. Lai, M. Awada, S. Floquet, C. Roch-Marchal, N. Watfa, J. Marrot, M. Haouas, F. Taulelle and E. Cadot, *Chem. Eur. J.*, 2015, **21**, 13311-13320.
31. O. Petina, D. Rehder, E. T. K. Haupt, A. Grego, I. A. Weinstock, A. Merca, H. Bögge, J. Szakács and A. Müller, *Angew. Chem. Int. Ed.*, 2010, **50**, 410-414.
32. S. Kopilevich, H. Gottlieb, K. Keinan-Adamsky, A. Müller and I. A. Weinstock, *Angew. Chem. Int. Ed.*, 2016, **55**, 4476-4481.
33. S. Kopilevich, A. Gil, M. Garcia-Ratés, J. Bonet-Ávalos, C. Bo, A. Müller and I. A. Weinstock, *J. Am. Chem. Soc.*, 2012, **134**, 13082-13088.
34. C. Besson, S. Schmitz, K. M. Capella, S. Kopilevich, I. A. Weinstock and P. Kögerler, *Dalton Trans.*, 2012, **41**, 9852.
35. N. A. G. Bandeira, S. Garai, A. Muller and C. Bo, *Chem. Commun.*, 2015, **51**, 15596-15599.
36. A. Rezaeifard, R. Haddad, M. Jafarpour and M. Hakimi, *J. Am. Chem. Soc.*, 2013, **135**, 10036-10039.
37. A. Nakhaei and A. Davoodnia, *Chin. J. Catal.*, 2014, **35**, 1761-1767.
38. A. Rezaeifard, R. Haddad, M. Jafarpour and M. Hakimi, *ACS Sustainable Chem. Eng.*, 2014, **2**, 942-950.
39. C. Yang, W. Zhao, Z. Cheng, B. Luo and D. Bi, *RSC Adv.*, 2015, **5**, 36809-36812.
40. A. Nakhaei, A. Davoodnia and A. Morsali, *Res. Chem. Int.*, 2015, **41**, 7815-7826.
41. A. Rezaeifard, M. Jafarpour, R. Haddad, H. Tavallaei and M. Hakimi, *J. Cluster Sci.*, 2015, **26**, 1439-1450.
42. E. Nikbakht, B. Yadollahi and M. R. Farsani, *Inorg. Chem. Comm.*, 2015, **55**, 135-138.
43. F. Jalilian, B. Yadollahi, M. R. Farsani, S. Tangestaninejad, H. A. Rudbari and R. Habibi, *Catal. Commun.*, 2015, **66**, 107-110.
44. H. Haddadi, E. Korani, S. Hafshejani and M. Farsani, *J. Cluster Sci.*, 2015, **26**, 1913-1922.
45. F. Jalilian, B. Yadollahi, M. Riahi Farsani, S. Tangestaninejad, H. Amiri Rudbari and R. Habibi, *RSC Adv.*, 2015, **5**, 70424-70428.
46. T. Mitra, P. Miro, A.-R. Tomsa, A. Merca, H. Bögge, J. B. Avalos, J. M. Poblet, C. Bo and A. Müller, *Chem. Eur. J.*, 2009, **15**, 1844-1852.
47. M. Garcia-Ratés, P. Miro, J. M. Poblet, C. Bo and J. B. Avalos, *J. Phys. Chem. B*, 2011, **115**, 5980-5992.
48. M. Garcia-Ratés, P. Miro, A. Müller, C. Bo and J. B. Avalos, *J. Phys. Chem. C*, 2014, **118**, 5545-5555.
49. E. Mani, E. Sanz, S. Roy, M. Dijkstra, J. Groenewold and W. K. Kegel, *J. Chem. Phys.*, 2012, **136**, 144706.
50. K. Goutham and E. Mani, *J. Mol. Eng. Mater.*, 2014, **02**, 1440005.
51. K. Kuepper, C. Derks, C. Taubitz, M. Prinz, L. Joly, J.-P. Kappler, A. Postnikov, W. Yang, T. V. Kuznetsova, U. Wiedwald, P. Ziemann and M. Neumann, *Dalton Trans.*, 2013, **42**, 7924-7935.
52. G. te Velde, F. M. Bickelhaupt, E. J. Baerends, C. Fonseca Guerra, S. J. A. van Gisbergen, J. G. Snijders and T. Ziegler, *J. Comput. Chem.*, 2001, **22**, 931-967.
53. R. Hoffmann, *Angew. Chem. Int. Ed.*, 1982, **21**, 711-724.
54. T. Ziegler and A. Rauk, *Inorg. Chem*, 1979, **18**, 1755-1759.
55. T. Ziegler and A. Rauk, *Inorg. Chem.*, 1979, **18**, 1558-1565.
56. F. M. Bickelhaupt, *J. Comput. Chem.*, 1999, **20**, 114-128.
57. K. Morokuma, *J. Chem. Phys.*, 1971, **55**, 1236-1244.
58. K. Kitaura and K. Morokuma, *Int. J. Quantum Chem*, 1976, **10**, 325-340.
59. M. v. Hopffgarten and G. Frenking, *Wiley Interdisciplinary Reviews: Computational Molecular Science*, 2012, **2**, 43-62.
60. G. Frenking, R. Tonner, S. Klein, N. Takagi, T. Shimizu, A. Krapp, K. K. Pandey and P. Parameswaran, *Chem. Soc. Rev.*, 2014, **43**, 5106-5139.
61. K. K. Pandey and R. Vishwakarma, *J. Organomet. Chem.*, 2016, **813**, 84-94.
62. K. K. Pandey, M. Lein and G. Frenking, *J. Am. Chem. Soc.*, 2003, **125**, 1660-1668.
63. P. Parameswaran and G. Frenking, *Chem. Eur. J.*, 2009, **15**, 8807-8816.
64. I. Fernández, G. Frenking and E. Uggerud, *Chem. Eur. J.*, 2009, **15**, 2166-2175.
65. W. J. van Zeist and F. M. Bickelhaupt, *Chemistry–A European Journal*, 2010, **16**, 5538-5541.
66. G. T. de Jong and F. M. Bickelhaupt, *Journal of Chemical Theory and Computation*, 2007, **3**, 514-529.
67. H. Abdoul-Carime, B. Farizon, M. Farizon, J.-C. Mulatier, J.-P. Dutasta and H. Chermette, *Physical Chemistry Chemical Physics*, 2015, **17**, 4448-4457.
68. C. F. Guerra, J. G. Snijders, G. te Velde and E. J. Baerends, *Theor. Chem. Acc.*, 1998, **99**, 391-403.
69. A. D. Becke, *J. Chem. Phys.*, 1993, **98**, 1372-1377.
70. J. P. Perdew, *Physical Review B*, 1986, **33**, 8822-8824.
71. J. P. Perdew, *Physical Review B*, 1986, **34**, 7406-7406.
72. E. van Lenthe, E. J. Baerends and J. G. Snijders, *J. Chem. Phys.*, 1994, **101**, 9783-9792.
73. E. van Lenthe, A. Ehlers and E.-J. Baerends, *J. Chem. Phys.*, 1999, **110**, 8943-8953.
74. A. Klamt and G. Schuurmann, *Journal of the Chemical Society , Perkin Transactions 2*, 1993, 799-805.
75. C. C. Pye and T. Ziegler, *Theor. Chem. Acc.*, 1999, **101**, 396-408.
76. N. L. Allinger, X. Zhou and J. Bergsma, *Journal of Molecular Structure-theochem*, 1994, **312**, 69-83.
77. http://dx.doi.org/10.19061/iochem-bd-1-4
78. M. Álvarez-Moreno, C. de Graaf, N. López, F. Maseras, J. M. Poblet and B. C, *J. Chem. Inf. Model.*, 2015, **55**, 95-103.
79. *Handbook of Chemistry and Physics*, 84th edn., CRC Press, 2003.
80. I. M. Kolthoff and P. J. Elving, *Treatise on analytical chemistry*, Interscience Encyclopedia, New York, 1959.